CHEMICAL ENGINEERING TRANSACTIONS
VOL. 97, 2022
A publication of AIDIC
The Italian Association of Chemical Engineering
Online at www.cetjournal.it
Guest Editors: Jeng Shiun Lim, Nor Alafiza Yunus, Jiří Jaromír Klemeš

ISBN 978-88-95608-96-9; **ISSN** 2283-9216
DOI: 10.3303/CET2297049

Excellent Charge Transfer over Highly Stable $LaCoO_3$ Perovskites for CO_2 Photoreduction to Solar Fuels under Visible Light

Mohamed Madi[a], Muhammad Tahir[b,*], Zaki Yamani Zakaria[a], Hajar Alias[a]

[a]Department of Chemical Reaction Engineering, School of Chemical and Energy Engineering, Universiti Teknologi Malaysia, 81310, UTM, Johor Bahru, Johor, Malaysia.
[b]Chemical and Petroleum Engineering Department, UAE University, P.O. Box 15551, Al Ain, United Arab Emirates
muhammad.tahir@uaeu.ac.ae

Global warming due to the combustion of fossil fuels has a major concern today. Therefore, the photocatalytic CO_2 reduction of valuable chemicals and fuels has become a hotly debated topic of study. This is due to the fact that this can simultaneously resolve the energy crisis and environmental issues. In this regard, a lot of research has gone into developing efficient photocatalysts for CO_2 reduction. Lanthanum cobalt perovskite ($LaCoO_3$) is one the semiconductors with catalytic capabilities, excellent stability, nontoxic, and low costs. The properties of $LaCoO_3$ perovskite based on the use of transition metals such as lanthanum (La) and cobalt (Co) make it applicable for photocatalytic enhancement of photoactivity. This is due to its visible light activity, ability to trap electrons, rapid charge carrier mobility, and conductivity. $LaCoO_3$ nanoparticles are synthesized through the hydrothermal technique. This study reveals that $LaCoO_3$ nanoparticles synthesized by hydrothermal method have a larger surface area and narrow bandgaps, resulting in a greater adsorptive capacity, increased visible light excitation, and an increase in the number of active sites for photocatalytic CO_2 reduction. The XRD, FTIR, and SEM was used to analyses the $LaCoO_3$ nanocatalysts. After 4 h with a 0.05 g catalyst loading and (CO_2 + water) as a reducing agent at normal temperature and pressure, the use of $LaCoO_3$ resulted in CO and CH_4 production rates of 110.4, and 28.5 mol g^{-1}. The high selectivity toward CO was certainly related to a greater surface area with enhanced light absorption. The $LaCoO_3$ photocatalyst was also investigated under a number of operating conditions, including photocatalyst loading, and reducing agents. Using three different catalyst loadings of 0.025, 0.05, and 0.1 g, the optimal catalyst loading was 0.05 g. Among the reducing agents, water favoured CO evolution, while the methanol-water system favoured CH_4 production. Interestingly, stability studies demonstrated that the $LaCoO_3$ perovskite behaved well and remained stable over numerous cycles without evident deterioration. Furthermore, a suggested photo-induced reaction mechanism was discussed. All of these results demonstrate that $LaCoO_3$ perovskite photocatalysts are capable of efficiently producing solar fuels and can be utilized in solar energy-related applications.

1. Introduction

As a result of global warming and energy issues, the conversion of CO_2 to valuable compounds and fuels has become an important research topic (Tahir and Tahir, 2022). During the last few years, the quest for technologies to recycle CO_2 as a natural resource has made artificial photosynthesis an appealing alternative. The photocatalytic solar conversion of CO_2 into value-added fuels or chemical compounds is among the most alluring approaches (Madi et al., 2021). Significant studies have been devoted to the development of efficient photocatalysts for the CO_2 reduction, such as TiO_2, g-C_3N_4, $CaFe_2O_4$, $InNbO_4$, and $LaCoO_3$ (Nguyen et al., 2020). Photocatalysts based on perovskite-type semiconductor materials are proven to be promising for converting CO_2 to solar fuels according to previous literature. This is because of their adjustable band gaps, optical and chemical stability, long lifetime of charge carrier, tunable crystal structure, and adequate oxygen vacancies. This made them a potential photocatalyst for the next generation and attracted a lot of researchers' attentions (Madi and Tahir, 2022).

Paper Received: 29 July 2022; Revised: 30 September 2022; Accepted: 6 October 2022
Please cite this article as: Madi M., Tahir M., Zakaria Z.Y., Alias H., 2022, Excellent Charge Transfer over Highly Stable LaCoO3 Perovskites for CO2 Photoreduction to Solar Fuels under Visible Light, Chemical Engineering Transactions, 97, 289-294 DOI:10.3303/CET2297049

Perovskite-type lanthanum cobaltate ($LaCoO_3$) as a low-cost catalyst is relatively rarely reported in the literature, in contrast to the aforementioned catalysts, and merits extensive research. According to Qin et al., the coralline-like $LaCoO_3$ material was synthesized using a citrate gel method and a subsequent thermal treatment in air for the photocatalytic conversion of CO_2 into CO under visible light irradiation (Qin et al., 2018). A $LaCoO_3$ photocatalyst was also successfully synthesized using sugarcane bagasse with a tunable oxygen vacancy for photocatalytic H_2 evolution in another study, according to Wu and colleagues (Wu et al., 2017).

$LaCoO_3$ is a perovskite oxide type (ABO_3) that exhibits a wide range of properties, including catalytic performance, adsorption activity, thermal stability, reducibility, electrical and electrocatalytic characteristics (Kumar et al., 2020).This is primarily attributable to their stable crystal structures, superior electromagnetic characteristics, and high catalytic activity for target reactions. In spite of this, it has been demonstrated that the preparation technique of $LaCoO_3$ significantly impacts its microstructure, catalytic performance, electrical and ionic conductivity, and consequently its potential applications. For instance, the development of dependable methods for generating nanoscale $LaCoO_3$ powders with a large specific surface area for use as electrocatalysts is a current subject of active research. Alternative methods for preparing $LaCoO_3$ samples that are finer and more homogeneous have been intensively investigated in attempt to overcome these limitations. Among them, the hydrothermal approach appears to be a promising method since it allows for the production of particles with controlled size and shape by adjusting synthesis parameters such as pH, temperature, reaction times, chemical reagent concentration, and solvent type (Tasleem et al., 2022).Comprehensive understanding of the creation of $LaCoO_3$ phase from the acquired precursors is highly desirable in order to gain control over the resultant physical features.

According to previous studies, Coralline-like $LaCoO_3$ perovskite materials are easy to make, and they can be employed as highly efficient and stable cocatalysts under the effect visible light irradiation to convert CO_2 onto CO, according to a study by Qin et al. (2018). Akhil et al. (2021) pointed out also that the polymerizable complex technique can be successfully used to prepare $LaCoO_3$ and use in many applications.

Although some research on $LaCoO_3$ nanopowders has been published, to the best of our knowledge, none of these works mention $LaCoO_3$ as a highly active catalyst for enhancing photochemical reduction of CO_2 to produce solar fuels under visible light illumination using the hydrothermal synthesis method. Several operating conditions, including photocatalyst loading, reducing agents, and stability analysis has been examined. The experimental data were used to propose the mechanism photocatalytic reaction process for CO_2 reduction to CO and CH_4. The current work is predictable to present an advanced solution for increasing the productivity of photocatalytic CO_2 reduction to solar fuels.

2. Experimental section

2.1 Materials

Sodium hydroxide (NaOH; Baker, 99.9 %), ammonium hydroxide (NH_4OH; Baker, 28.0–30.0 %), (La $(NO_3)_3.6H_2O$; Aldrich, 99.99 %), cobalt (II) nitrate hexahydrate (Co $(NO_3)_2.6H_2O$; Aldrich, 99.9 %), Methanol (Merck, AR 99.9 %), and distilled water have been used as supplied without further purification in this study.

2.2 Synthesis of $LaCoO_3$ nanoparticles

The hydrothermal method could be used to synthesize $LaCoO_3$ nanoparticles. To begin, 40 mL of pure distilled water is mixed with 1.11 mL of ammonium hydroxide (NH_4OH, Sigma Aldrich, 33 %) and agitated for 30 min until it is uniform in texture. Second, an equimolar molar ratio of 1:1 was used to combine 0.86 g of La $(NO_3)_3$. 6 H_2O with 0.58 g of Co $(NO_3)_2.6H_2O$. With 40 min of vigorous stirring, NaOH is added to the mixture. Third, a reaction solution in a stainless-steel Teflon-lined vessel is heated for 48 h at 180 °C in a muffle furnace. The products were centrifuged and diluted multiple times with distilled water till pH=7 to reduce alkalinity and eliminate unreacted compounds after the mixture was cooled to room temperature. The hydrothermally produced precursor powder was finally calcined for 2 h at 850 °C in an alumina crucible in order to get the crystalline phase of $LaCoO_3$.

2.3 Characterization

Analysis of pure $LaCoO_3$ was carried out using XRD (Bruker Advance D8, 40 mA, 40 kV) with Cu K radiation (λ =0.154 nm) to determine the crystalline phase and structure change. The Fourier transform infrared spectroscopy (FTIR) (model Shimadzu, IRTracer-100) was used to investigate the presence of specific functional groups in nanostructures. Using an Agilent Cary 100 UV-vis spectrophotometer, we determined the UV-visible diffuse reflectance spectra (DRS) of the powder samples. Using a scanning electron microscope (SEM, Hitachi SU8020), the surface morphology and structure of material was also characterized.

2.4 Photoactivity test

The fixed bed photoreactor is comprised of an 80 cm^3 stainless-steel cylindrical tank with a length of 5 cm as shown in Figure 1. A 10 mm thick Pyrex glass was used to pass light through, and a parabolic-shaped reflector was used to guide light into the photoreactor room. A 35W HID Xe lamp with a power density of 20 mW/cm^2 was also employed to produce visible light. After the photoreactor chamber was purged with purified helium (He) flow, a mixture of gases (CO_2, H_2O, and He) was regularly pumped through the reactor for one hour to saturate the catalyst. For offline analysis, gas components were obtained at regular intervals using a gastight syringe (Agilent, 1,000 L). The gas products were analyzed using a Gas Chromatograph (GC, 6890). With two detectors, the FID and TCD as well as Carboxen 1010 PLOT capillary column in the GC, the gas chromatograph was capable of providing high accurate results.

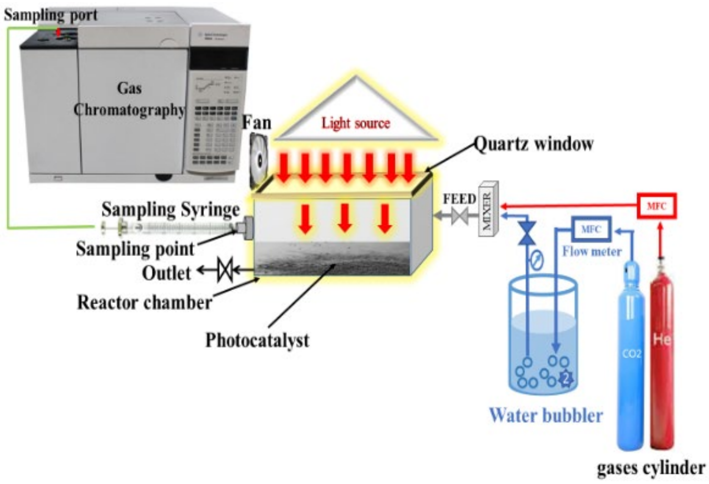

Figure 1: Schematic demonstration of the experimental setup in a fixed bed photoreactor

3. Results and discussion

3.1 Characterization of samples

The diffraction peaks of pure $LaCoO_3$ were positioned at 23.1 ° , 32.6 °, 33.1 °, 40.5 °, 41.1 °,and 47.3 °, 68.9 °, 69.8 °,78.6 °, 79.4 °,and 87.9 ° corresponding to the (012), (110), (104), (202), (006), (024), (220), (208), (134), (128), and (404) planes, which is in accordance with JCPDS no. 48-0123 (Madi & Tahir, 2022). According to existing research, the diffraction peaks of pure $LaCoO_3$ were compatible with the results of previous literature (Sadabadi et al., 2021).This prove the successful synthesis of $LoCoO_3$ nanoparticles as shown in Figure 2a.
Figure 2b depicts the FTIR for $LaCoO_3$, which reveals dips at 598, and 590 cm^{-1} that suggest the production of $LaCoO_3$ due to the vibration of the metal oxygen band. More importantly, the FTIR bands at 1627, 1530, 1423, 1053 ,and 3650 cm^{-1} correspond to the $LaCoO_3$ lattice vibration (Surendar et al., 2016).
Through the correlation between $(hv)^2$ and photon energy Tauc plots, the energy band gap of $LaCoO_3$ was determined and calculated using the Tauc plot, and the Kubelka-Munk (KM) function as shown in Figure 2c. The absorption coefficient of the material (α) was defined as in Eq(1), while the nature of the semiconductor (r) was defined as in Eq(2). $LaCoO_3$ was found to have band energies of 1.51 eV. The correlation between Eg, CB, and VB is depicted in Eq(2), the CB calculation can be determined from Eq(3). Where X is the coefficient for semiconductor electronegativity (EN), E is the energy-free electron, and Eg is the semiconductor band gap. On the hydrogen scale, E^e is the energy of free electrons (4.5 eV vs NHE), E_g is the semiconductor band gap energy, χ is the electronegativity of $LaCoO_3$ photocatalyst which is about 4.63 eV (Madi and Tahir, 2022).

$$E_g = (\alpha h v)^{\frac{1}{r}} \tag{1}$$

$$E_g = VB - CB \tag{2}$$

$$CB = X - E - 0.5E_g \tag{3}$$

The SEM examines the morphologies and microstructures of the as-fabricated $LaCoO_3$ sample as shown in Figure 2d. The increased calcination temperature resulted in the development of polycrystals with bigger particle sizes. However, despite the higher calcination temperature, less aggregation occurred. According to the literature, a porous hierarchical structure has the potential to absorb more light and has a more active site for carrying out a reduction reaction, as well as a more improved charge transfer (Wang et al., 2020).

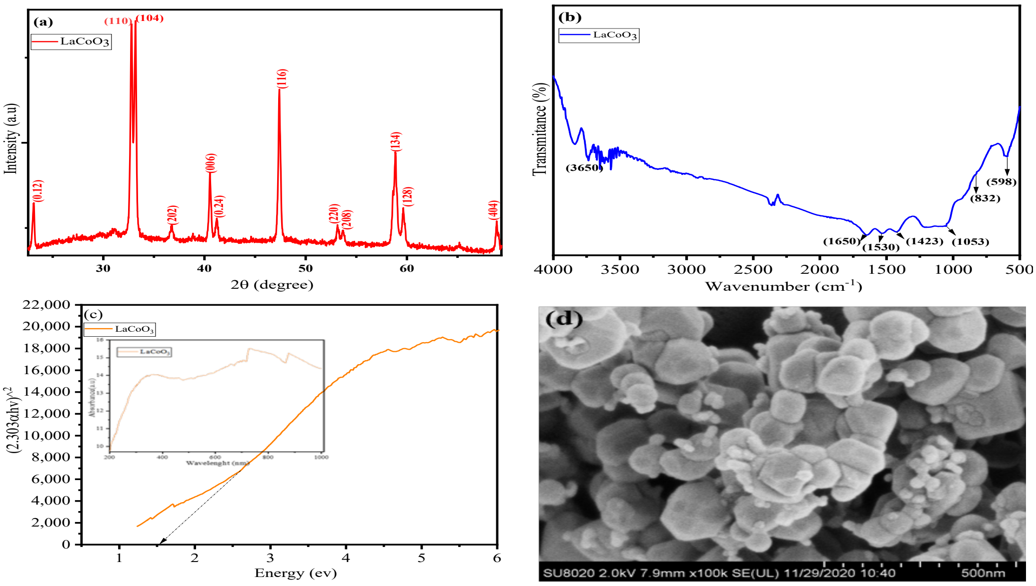

Figure 2: (a) XRD patterns, (b) FTIR Spectra, (c) UV–vis spectrum and Tauc plot, (d) SEM analysis

3.2 Photocatalytic CO_2 reduction

The only way that molecules containing carbon could have been produced was through CO_2 photo-reduction, and all experiments that have been utilised to confirm the production of every component have shown that CO is the most abundant CO_2 photo-reduction result.

At three different amounts of photocatalyst (0.025, 0.05, and 0.1 g), the efficiency of $LaCoO_3$ perovskite was tested as shown in Figure 3a. This is due to the fact that varied catalyst loading is clearly entirely responsible for the increase or decrease in the production rate and selectivity. After 4 h with a 0.5 g catalyst loading, the optimal production values for CO and CH_4 were observed to be 110.4 and 28.5 µmol g^{-1}. At higher catalyst loading, the results decrease due to the agglomeration (particle-particle interaction) of catalyst nanoparticles, which restrict passage of light and results in poor light absorption. Conversely, at lower catalyst loading, the results also decrease because there is less active surface available for activating photocatalytic CO_2 reduction under the same reaction conditions.

As shown in Figure 3b, different reducing agents were used for photocatalytic CO_2 reduction as the (CO_2 + water) system favored CO development while the methanol-water system favored CH_4 evolution. The optimal production value for CO was 110.4 µmol g^{-1} using CO_2-water system, while the optimal production values for CH_4 was 70 µmol g^{-1} using methanol–water mixture (CO_2 + 5 % Methanol). When methanol was introduced into the feed mixture, CH_4 production rate was increased. This is not only encouraging more production of protons, but also provides electrons during oxidation process. All of these results show that catalyst loading, and reducing agents have a considerable impact on both the product's yield and selectivity. Due to the paucity of research on the conversion of carbon dioxide to solar energy, this study has been compared to a similar study. The current study found that CO production after 4 h were 3.8 times higher than those seen in a previous study after half an hour(Qin et al., 2018).

As displayed in Figure 3c, the stability test of the $LaCoO_3$ photocatalysts exhibited a continuous production of CO and CH_4 in several cycles with no noticeable deactivation under visible light. The photoreactor was irradiated for 4 h after being cleaned and purged with nitrogen gas, then saturated with water-humidified CO_2 gas for 1 h in each cycle. Both CO and CH_4 production were high in the first cycle and dropped in the second cycle, while both CO and CH_4 production in the third cycle was practically identical to the second cycle. This decline in yield in 2nd cycle could be a result of a reduction in the adsorption of CO_2 on the catalyst's surface. The photoactivity reduction was very small, indicating that the catalyst deactivation is very minor and that the photocatalyst has excellent performance.

3.3 Photocatalytic mechanism for CO_2 reduction

CO_2 reacts with H_2O in order to produce CO and lower amounts of CH_4 as the probable products over $LaCoO_3$ sample during photocatalytic CO_2 reduction with water. A mechanism is demonstrated in Eq(4) to Eq(8) (Tahir et al., 2021).

$$\mathrm{LaCoO_3 + hv \rightarrow\ LaCoO_3\,(\,h^+\ +\ e^-)} \tag{4}$$

$$\mathrm{2H_2O + 4h^+ \rightarrow\ O_2\ +\ 4H^+} \tag{5}$$

$$\mathrm{CO_2 + e^- \rightarrow CO^{\bullet -}} \tag{6}$$

$$\mathrm{CO_2 + 2H^+ +\ 2e^- \rightarrow CO\ +\ H_2O} \tag{7}$$

$$\mathrm{CO_2 + 8H^+ +\ 8e^- \rightarrow CH_4\ +\ 2H_2O} \tag{8}$$

Perovskite $LaCoO_3$ absorbs light irradiation energy within a visible light range equivalent to or greater than its band gap. The photoinduced electrons will travel from the VB to the CB of $LaCoO_3$, while the holes remained in the VB and produced a large number of electron-hole pairs (Eq(4)). $LaCoO_3$ has holes at the VB that will be oxidized by water to create H^+, as depicted in Eq(5). As demonstrated in Eq(6), the electrons are transported to the surface of $LaCoO_3$, and it interacts with CO_2 to create $^{\bullet}CO$ radicals (6). Finally, the formation of CO and CH_4 is achieved by involving 2 and 8 electrons, as shown in Eq(7) and Eq(8). The reaction process for photocatalytic CO_2 reduction with H_2O to fuels is demonstrated in Figure 3d.

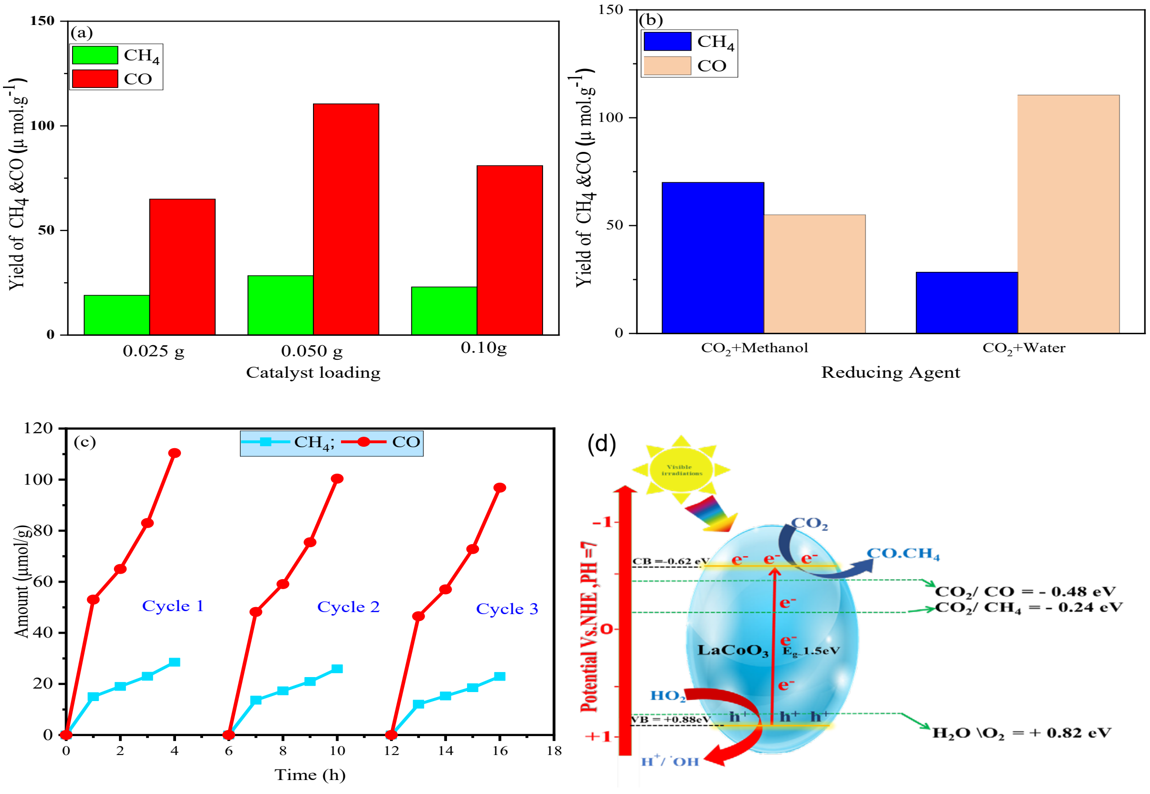

Figure 3: (a) Catalyst loading of $LaCoO_3$ (b) Reducing Agent of $LaCoO_3$ (c) Stability of $LaCoO_3$, (d) Photocatalytic electron transfer mechanism in $LaCoO_3$ nanocomposite

4. Conclusions

It has been concluded that hydrothermal synthesis of $LaCoO_3$ perovskite material has been successfully synthesized with higher photocatalytic efficiency under visible light irradiation. The synthesized $LaCoO_3$ material with the hydrothermal method was shown a higher surface area and narrow band gap. $LaCoO_3$ is shown as a highly efficient and stable photocatalyst for reducing CO_2 with water as the reducing agent to CO and CH_4 under visible-light irradiation. The photocatalytic CO evolution of the $LaCoO_3$ nanoparticle was 110.4 mole $g^{-1}h^{-1}$ with catalyst loading of 0.05 g was approximately 1.7 and 1.36-fold larger than the catalyst loading at 0.025 and 0.1

g. The CO production is also 3.8-fold higher than the amount of CH_4 produced under the same irradiation time. The efficiency of $LaCoO_3$ perovskite under a variety of aspects, including catalyst loading and reducing agents has different effects. Among the sacrificial reagents, methanol-water system found more promising for CO_2 reduction to CH_4. Pure water was favorable for more CO evolution under the same operating conditions. In addition, Optimized catalyst loading of 0.05 g found best for maximizing the photocatalytic efficiency. Perovskite based photocatalyst was found stable for continuous CO_2 evolution in multiple cycles. This research holds significant promise for perovskite as a material for the development of advanced CO_2 reduction systems.

Acknowledgement

The authors would like to extend their most profound appreciation to Ministry of Higher Education for the financial support under Fundamental Research Grant Scheme (FRGS) number: FRGS/1/2020/TK0/UTM/02/84 and UTM Fundamental Research Grant number: Q.J130000.2551.20H92 for funding this project.

References

Akhil S., Kusuma J., Akash S.,Geetha Balakrishna R., 2021, Perovskite-like ceramic hole transport material for quantum dot sensitized solar cells, Applied Solar Energy, 224, 355-360.

Kumar A., Kumar A., Krishnan V., 2020, Perovskite oxide based materials for energy and environment-oriented photocatalysis, ACS Catalysis, 10(17), 10253-10315.

Madi M., Tahir M., 2022, Highly stable $LaCoO_3$ perovskite supported g-C_3N_4 nanotextures with proficient charges migration for visible light CO_2 photoreduction to CO and CH_4, Materials Science in Semiconductor Processing, 142, 106517.

Madi M., Tahir M., Tasleem S., 2021, Advances in structural modification of perovskite semiconductors for visible light assisted photocatalytic CO_2 reduction to renewable solar fuels: A review, Journal of Environmental Chemical Engineering, 9(5), 106264.

Nguyen V.H., Nguyen B.S., Jin Z., Shokouhimehr M., Jang H.W., Hu C., Singh P., Raizada P., Peng W., Shiung Lam S., Xia C., Nguyen C.C., Kim S.Y., Le Q.V., 2020, Towards artificial photosynthesis: Sustainable hydrogen utilization for photocatalytic reduction of CO_2 to high-value renewable fuels, Chemical Engineering Journal, 402, 126184.

Qin J., Lin L., Wang X., 2018, A perovskite oxide $LaCoO_3$ cocatalyst for efficient photocatalytic reduction of CO_2 with visible light, Chemical Communications, 54(18), 2272-2275.

Sadabadi H., Allahkaram S.R., Kordijazi A., Akbarzadeh O., Rohatgi P.K., 2021, Structural characterization of $LaCoO_3$ perovskite nanoparticles synthesized by sol–gel autocombustion method, Engineering Reports, 3(6), e12335.

Surendar M., Sagar T.V., Raveendra G., Ashwani Kumar M., Lingaiah N., Rama Rao K.S.,Sai Prasad P.S., 2016, Pt doped $LaCoO_3$ perovskite: A precursor for a highly efficient catalyst for hydrogen production from glycerol, International Journal of Hydrogen Energy, 41(4), 2285-2297.

Tahir B., Tahir M., Nawawi M.G.M., 2021, Synthesis of WO_3/g-C_3N_4 nanocomposite for photocatalytic CO_2 reduction under visible light, Chemical Engineering Transactions, 83, 247-252.

Tahir M., Tahir B., 2022, Constructing S-scheme 2D/0D g-C_3N_4/TiO_2 NPs/MPs heterojunction with 2D-Ti_3AlC_2 MAX cocatalyst for photocatalytic CO_2 reduction to CO/CH_4 in fixed-bed and monolith photoreactors, Journal of Materials Science & Technology, 106, 195-210.

Tasleem S., Tahir M., Zakaria Z.Y, 2022, Z-scheme Ag-NPs-embedded $LaCoO_3$ dispersed pCN heterojunction with higher kinetic rate for stimulating photocatalytic solar H_2 production, Energy Conversion and Management, 266, 115787.

Wang R., Ye C., Wang H., Jiang F, 2020, Z-Scheme $LaCoO_3$/g-C_3N_4 for Efficient Full-Spectrum Light-Simulated Solar Photocatalytic Hydrogen Generation, ACS omega, *5*(47), 30373-30382.

Wu M., Luo M., Guo M., Jia L., 2017, Sugarcane Bagasse hydrolysis by metal ions mediated synthesis of perovskite $LaCoO_3$ and the photocatalytic performance for hydrogen from formaldehyde solution under visible light, ACS Sustainable Chemistry & Engineering*, 5*(12), 11558-11565.